Dalton Transactions

ROYAL SOCIETY OF CHEMISTRY

COMMUNICATION

View Article Online
View Journal | View Issue

Cite this: *Dalton Trans.*, 2023, **52**, 14324

Received 25th September 2023,
Accepted 27th September 2023

DOI: 10.1039/d3dt03151a

rsc.li/dalton

CuO metallic aerogels with a tailored nodular morphology

Lucía dos Santos-Gómez, *†[a] Natalia Rey-Raap,[b] S. García-Granda [c] and Ana Arenillas[b]

This work reports, for the first time, an efficient and fast microwave-based method for the preparation of CuO aerogels. For that, $CuCl_2$, glyoxylic acid and sodium carbonate are employed as reagents. Different experimental conditions such as synthesis temperature, synthesis time and concentration of the precursor solution are investigated to design CuO aerogels with customizable nodular morphologies. The resulting aerogels exhibit well-defined three-dimensional structures and nodular sizes, and therefore, textural properties vary according to the experimental parameters applied in their synthesis.

1. Introduction

Aerogels are large surface area materials composed of building block networks, which form a highly porous architecture.[1] The synthesis of aerogels has been investigated for several years.[2] Initial approaches to prepare metallic aerogels began with the combustion synthesis, but controlling their structure and shape was difficult and involved costly procedures and energetic materials.[3] Next, hybrid oxide aerogels have been infiltrated with aromatic polymers that can be smelted, forming metallic aerogels.[4] Again, controlling the nanoscale structure and morphology is challenging because of the elevated temperatures employed for smelting the oxides. More recently, the synthesis method of metallic aerogels involved the gelation of metal nanoparticles.[5] Normally, the sol–gel approach employs alkoxide-based precursors to form the metal oxide gel. However, this procedure is not appropriate for synthesizing metallic gels with low valence metals such as CuO,[6] NiO[7] and ZnO,[8] because the freedom of metal ion growth is limited. Currently, self-assembly is a usual bottom-up method that has attracted attention for the preparation of remarkable structures. In this, metal nanoparticles act as building blocks to fabricate porous 3D frameworks.[9] Such nanostructures not only possess the chemical and physical properties of the materials but also desirable characteristics in terms of their size, morphology and composition.

CuO nanoparticles have drawn the attention of the scientific community due to their excellent potential application in several areas such as catalysis, energy conversion/storage and electrochemical sensors. For instance, Poreddy *et al.* utilized CuO as a cost-effective and highly selective catalyst to generate carbonyl compounds through the oxidative dehydrogenation of alcohols.[10] Gamarra *et al.* investigated CuO/CeO_2 catalysts for the preferential oxidation of CO.[11] Li *et al.* reported a highly responsive and durable CuO-based biosensor to enhance the detection sensitivity of xanthine oxidase's activity.[12] Nevertheless, the synthesis of a CuO aerogel is challenging because nanoparticles promote low surface areas to reduce surface energy. For example, some investigations have been reported in the literature for preparing CuO aerogels, but the synthesis method used is complicated and time-consuming, ranging from several days to several weeks.[4,13–15] Moreover, the diversity of the morphologies of CuO aerogels needs to be controlled by developing new procedures for gel formation so that aerogels with different shapes or structures can be obtained. Also, controlling the porous properties of these aerogels, such as surface area and porosity, is of great importance for their future implementation. Recently, Martínez-Lázaro *et al.* have reported an efficient microwave-assisted procedure for the preparation of Pd aerogels.[16] The resulting material presented higher electrochemically active surface area than those prepared by conventional heating. Nevertheless, this procedure has never been investigated for copper-based aerogels.

Based on the above concerns, we demonstrate, for the first time, a simple method for the formation of CuO aerogels with

[a]*Universidad de Málaga, Dpto. de Química Inorgánica, Cristalografía y Mineralogía, 29071-Málaga, Spain. E-mail: ldsg@uma.es*
[b]*Instituto de Ciencia y Tecnología del Carbono, INCAR-CSIC, 33011-Oviedo, Spain*
[c]*Department of Physical and Analytical Chemistry, University of Oviedo (CINN-CSIC), 33006-Oviedo, Spain*
†Present address: Dpto. de Química Inorgánica, Cristalografía y Mineralogía, Facultad de Ciencias, Campus de Teatinos, Universidad de Málaga, 29071-Málaga, Spain.

well-defined nanostructures by employing microwave heating. Several experimental conditions are tested to design CuO aerogels with widely customizable nodular morphologies. In addition, the porous properties of these materials are thoroughly investigated.

2. Experimental

2.1. Synthesis of materials

CuO aerogels were prepared by the one-pot synthesis method. As an example, 200 mL of precursor solution was prepared by mixing 40 mL of metallic solution and 160 mL of reducing solution (volume ratio 1 : 4). The metallic solution was prepared by dissolving 0.08 g of $CuCl_2$ (99%, Sigma-Aldrich) in Milli-Q water. The reducing solution was made by dissolving (in a weight ratio 1 : 6) 0.16 g of glyoxylic acid (98%, Sigma-Aldrich) and 0.96 g of sodium carbonate (Indspec, 99%) in Milli-Q water. The concentration of such precursor solution was 0.06 mol L^{-1}. A precursor solution 5 times more concentrated than the previous one was also prepared by mixing the same volume of metallic and reducing solutions (40 mL and 160 mL, respectively), but, in this case, these solutions contained 0.40 g of $CuCl_2$, 0.80 g of glyoxylic acid and 4.80 g of sodium carbonate. Similarly, a precursor solution 10 times more concentrated than the original one was used, which contained 0.80 g of $CuCl_2$, 1.60 g of glyoxylic acid and 9.60 g of sodium carbonate.

The resulting precursor solutions were heated at different temperatures, from 45 to 90 °C, for times ranging from 4.5 to 9 h, in a microwave oven. This offers a significant advantage in contrast to the typical heating techniques used in conventional synthesis methods. After that, the hydrogels were washed with an excess of Milli-Q water several times to remove the remaining residues such as the excess ions and unreacted organic solvent. Then, the hydrogels were frozen in liquid N_2 and dehydrated by freeze drying for 24 h. Hereinafter, the resulting copper aerogels (CuA) will be labelled as CuA-*T*/*t*-*C*, where *T* indicates the synthesis temperature, *t* the synthesis time and *C* the concentration of the precursor solution (1*x*, 5*x* and 10*x*). For comparison purposes, another CuO gel was prepared following the same protocol but using a conventional heating source. The synthesis temperature and the concentration of the precursor solution were fixed at 45 °C and 1*x*, respectively. Under these conditions, it took 36 h to synthesize a CuO aerogel, whereas the microwave-assisted preparation required only 9 h for an equivalent sample. Thus, this microwave-based procedure achieves a 75% reduction in synthesis time.

2.2. Structural and morphological characterization

The crystal structures were studied by XRD in a D8 Advance diffractometer (Bruker) with Cu $K_{\alpha 1}$ radiation. The X'Pert HighScore Plus program was employed for phase identification.[17] N_2 adsorption/desorption isotherms were measured at −196 °C in a Tristar 3020 instrument (Micromeritics). The specific surface area (S_{BET}) was calculated applying the Brunauer–Emmett–Teller equation. The volume of micropores was determined with the Dubinin–Radushkevich equation. The N_2 adsorbed at the saturation point was employed to determine the total pore volume. The morphology and microstructure of the metallic aerogels were examined by SEM in a Quanta FEG 650 microscope.

3. Results and discussion

3.1. Gelation mechanism and structural and textural properties

The microwave-based approach proposed in this work shows considerable advantages for rapid and tuneable gelation. As shown in Fig. 1a, the initial blue colour of the precursor solution turns brown, in a vertical gradient, and lastly forms a flexible hydrogel at the bottom of a transparent colourless solution in a few hours (Fig. 1b). This phenomenon can be explained by the assumption of the Derjaguin–Landau–Verwey–Overbeek (DLVO) theory, where different ions increase the ionic strength and, therefore, the electrostatically charged particles induce aggregation.[18,19] After that, the initiated aggregates grow gradually and precipitate due to the gravity, following the gravity-driven assembly model. As a result, a brown monolithic gel with a porous 3D microstructure is obtained (Fig. 1c and d).

Fig. 1e shows the X-ray powder diffraction (XRPD) patterns of CuA-90/4.5-1*x* as a representative example of the series, as no significant differences between samples were detected. This fact indicates that the process variables studied do not influence the chemical nature of the aerogels. The observed peaks are broad because of the nano-size of the crystalline particles. Two main peaks are observed at 35° and 38° (2 θ), assigned to the (002) and (111) reflections of CuO, respectively (JCPDS no. 48-1548). The other reflections of CuO are also clearly visible, indicating that the CuO aerogel, with a monoclinic structure, has been successfully synthesized. No extra peaks ascribed to secondary phases are detected. The size of CuO nanoparticles can be determined by the broadening diffraction peaks of the XRPD patterns. Thus, the crystallite size was calculated using the Scherrer's equation, obtaining a particle size of about 14 nm. On the other hand, the aerogel prepared by conventional heating presents a mixture of CuO and Cu_2O phases. This could be attributed to the extended synthesis time, which might encourage the blending of various oxidation states of copper. Conventional heating is not as homogeneous as microwave heating, which provides a purer material without phase mixtures. The presence of Cu_2O can pose drawbacks in certain applications. For instance, Cu_2O is not suitable as an electrocatalyst for the oxygen reduction reaction.[2] In contrast, the strong affinity of Cu^{2+} ions for creating stable complexes with nitrogen-based ligands makes this an interesting strategy for enhancing the electrocatalytic performance of CuO.[20]

Controlling the porosity and the surface area of the metallic aerogels is of great importance. The porous properties of the aerogels were investigated by N_2 adsorption at −196 °C. Fig. 1f

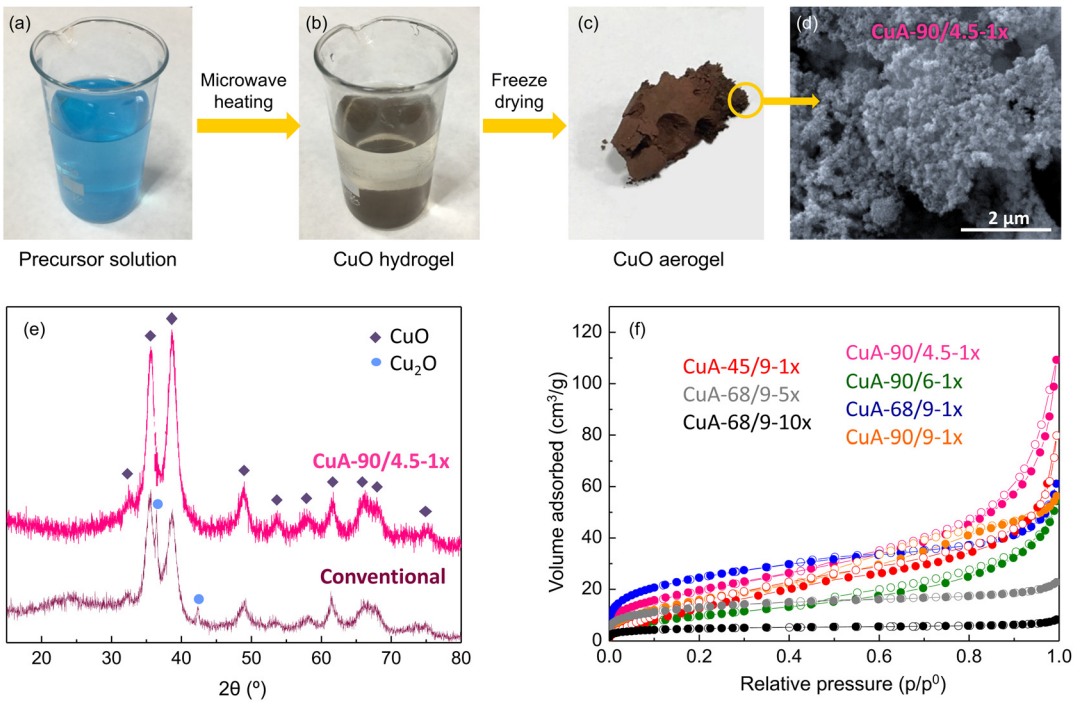

Fig. 1 (a–c) Photographs of the synthesis procedure of CuO aerogels. (d) SEM image of the CuA-90/4.5-1*x* aerogel. (e) XRD patterns of CuA-90/4.5-1*x* and the aerogel prepared by conventional heating. (f) N_2 adsorption–desorption isotherms for the CuO aerogels.

displays the adsorption–desorption N_2 isotherms of all the prepared samples, which correspond to reversible type II isotherms according to the IUPAC classification, related to macroporous solids. In general terms, the isotherms present a low increase of adsorption at low relative pressures, which means low micropore volume (Table 1). At relative pressures near saturation, the amount of N_2 adsorbed increases, which is a characteristic behaviour of macroporous materials. Some aerogels also present an increase in the adsorbed volume in the intermediate range of partial pressures, which indicates the presence of porosity in the range of mesopores. The specific surface area (S_{BET}) and external surface area (S_{ext}) values are included in Table 1. The surface areas of all prepared samples are in agreement with those of related materials,[5] and the highest value is presented by the CuA-68/9-1*x* sample, with S_{BET} and S_{ext} of 89 and 86 $m^2\ g^{-1}$, respectively. It is worth noting that S_{ext} is an important parameter for several applications, such as catalysis, where there is a heterogeneous interaction with these materials. The S_{ext} values are very close to the S_{BET} for all samples, suggesting that nearly all specific surface areas of these samples are quite accessible.

Textural characterization indicates that synthesis conditions influence the final porosity developed by the aerogels. The microporosity decreases on increasing the concentration of the precursor solution (Table 1), while the mesoporosity decreases. The shape of the isotherms suggests that the samples evolved from mesoporous to microporous materials on increasing the concentration of the precursor solution (Fig. 1f), which will be later confirmed by the SEM images shown in Fig. 2. On the other hand, it seems that the temperature and time of synthesis hardly modify the microporosity but influence the mesoporosity of the samples, as the volume of mesopores decreases on increasing temperature and time, suggesting, once again, that the samples evolved from mesoporous to macroporous materials. This fact could be related to the enhancement of the reactions occurring, and therefore the increase of the nodule's size with the temperature. As the meso/microporosity is defined as the space between nodules,

Table 1 Synthesis conditions and textural properties of the CuO aerogels

Sample	T (°C)	Time (h)	Concentration	S_{BET} ($m^2\ g^{-1}$)	S_{ext} ($m^2\ g^{-1}$)	V_{micro} ($cm^3\ g^{-1}$)	V_{meso} ($cm^3\ g^{-1}$)	V_{total} ($cm^3\ g^{-1}$)
CuA-45/9-1*x*	45	9	*x*1	61	59	0.01	0.11	0.12
CuA-68/9-1*x*	68	9	*x*1	89	86	0.02	0.08	0.10
CuA-68/9-5*x*	68	9	*x*5	47	42	0.01	0.03	0.04
CuA-68/9-10*x*	68	9	*x*10	18	15	0.01	0.00	0.01
CuA-90/4.5-1*x*	90	4.5	*x*1	74	71	0.02	0.15	0.17
CuA-90/6-1*x*	90	6	*x*1	39	38	0.01	0.07	0.08
CuA-90/9-1*x*	90	9	*x*1	62	60	0.01	0.08	0.09

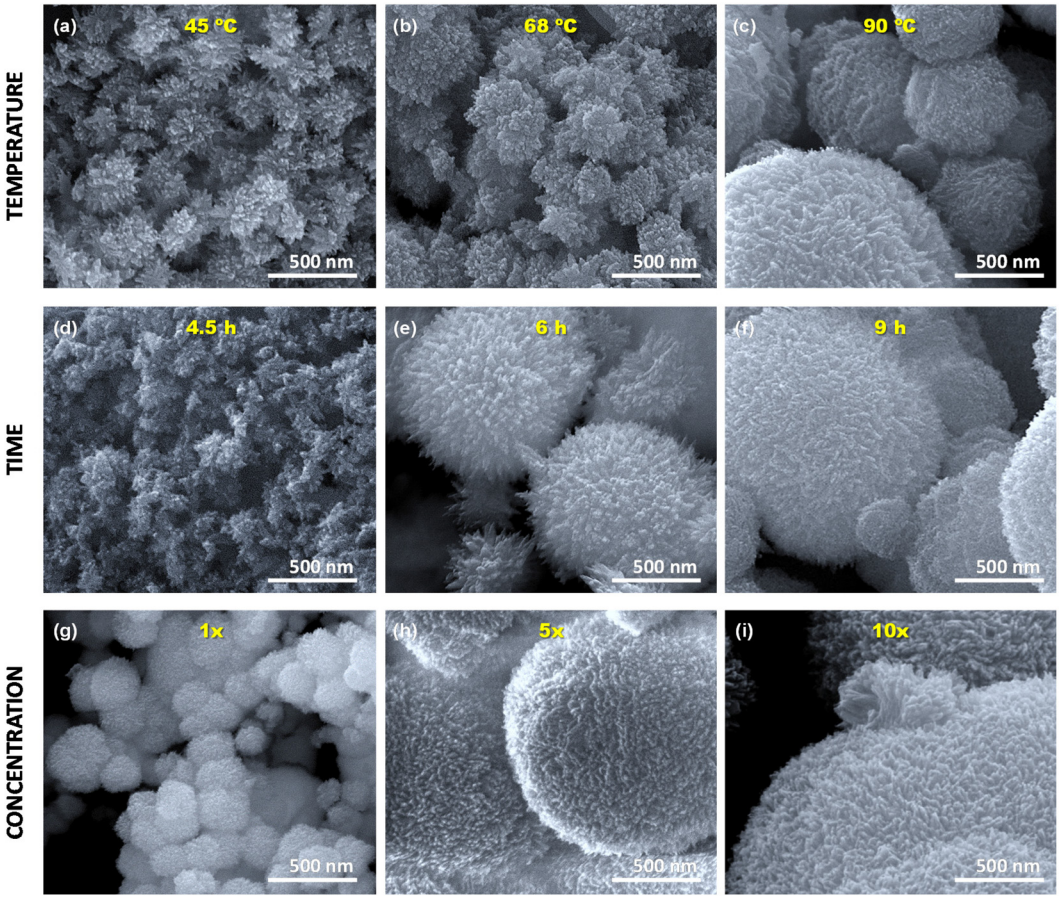

Fig. 2 SEM images of the CuO aerogels prepared at different (a–c) temperatures, (d–f) times and (g–i) concentrations of the precursor solution.

the size of the pores increases also with temperature. The time of synthesis has a less clear influence on the final porous properties; this could be due to the interdependence on other variables or maybe because its influence is mainly on macroporosity. It should be noted that the macropores cannot be determined by N_2 adsorption, and mercury porosimetry should be carried out instead. However, it is not possible to perform mercury porosimetry since these materials cannot withstand the operating pressure used in this technique and they crumble into a powder, hindering their appropriate characterization. Nevertheless, large macropores can be evaluated by SEM.

3.2. Morphological characterization

Fig. 2 shows the SEM images of the CuO aerogels. Three different experimental parameters, such as operating temperature, time, and concentration of reactants, are investigated to know their effect on the morphology of the samples. All samples possess a similar nodular morphology with a 3D open microstructure since, after the formation of the initial colloids, they aggregate and grow in all directions, forming nodular structures. The nodular structure is the morphology that presents the maximum surface area, which can favour their application in certain catalytic reactions. Moreover, the use of microwave radiation technology allows the preparation of the CuO aerogels not only saving processing time but also obtaining materials with homogeneous and controlled particle sizes, unlike current CuO aerogel synthesis methods. This is due to the fact that microwave radiation heats the bulk of the precursor solution without a temperature gradient, which favours homogeneous reactions and the excellent dispersion of the nucleation points.[16] These initial structures grow up homogeneously, thus controlling the final size of the nodules.

Different nodular sizes are distinguished according to the conditions applied during their synthesis. For example, the nodular sizes increase with the temperature of heating (Fig. 2a–c). Samples heated at 45, 68 and 90 °C present a nodular size of about 200, 400 and 700 nm, respectively. This is attributed to the increase of the kinetic energy of the copper nanoparticles with temperature, increasing the speed with which they join the nodules and, therefore, larger nodules are obtained. Regarding the synthesis time, there is a positive correlation between the nodule sizes and the sedimentation time. It means that the number of particles that merge into the nodules increases with time. The sizes of the nodules vary from 100 nm to 1.5 μm when the synthesis time increases from 4.5 to 9 h, respectively (Fig. 2d–f). Finally, the concentration of the precursor solution also affects the nodular size

of the CuO aerogels, ranging from 200 nm to several microns when the concentration of the precursor solution is increased by 10 times. This may be explained by the higher number of initial nucleation points present in the solution with higher concentration. Moreover, there is a greater number of copper nanoparticles in the precursor solution that can attach the nodules, increasing their size. These results are in agreement with those obtained from N2 adsorption–desorption isotherms in which it was observed that the samples evolved from mesoporous to macroporous materials on increasing the concentration of the precursor solution, and time and temperature of synthesis.

4. Conclusions

CuO aerogels have been synthesized by a one-pot, simple and fast microwave-based approach. Several experimental conditions have been tested to design CuO aerogels with well-controlled and homogeneous shapes. Aerogels exhibited well-defined three-dimensional nodular structures. The nodular size increases with the synthesis temperature, the synthesis time, and the concentration of the precursor solution, which involves an evolution of the porous structures from mesoporosity to macroporosity. Therefore, CuO aerogels with similar chemical composition and controlled morphology and porosity can be obtained by varying the experimental synthesis conditions.

Conflicts of interest

There are no conflicts to declare.

Acknowledgements

This work was supported by the PID2020-113001RB-100 project, funded by Ministerio de Ciencia e Innovación (MCIN) (MCIN/AEI/10.13039/501100011033) and by the European Union NextGenerationEU/PRTR; MCIN-21-PID2020-113558RB-C41 project, funded by MCIN and the projects from Principado de Asturias (GRUPIN2021 IDI/2021/50921 and SV-PA-21-AYUD/2021/50997). L. d. S. G. thanks the Universidad de Málaga for the funding. N. R. R. is grateful to the Horizon-MSCA-2021-PF-01-01 call for financial support through the Metgel project 101059852.

References

1 A. C. Pierre and G. M. Pajonk, *Chem. Rev.*, 2002, **102**, 4243–4266.
2 K. A. Adegoke and N. W. Maxakato, *Coord. Chem. Rev.*, 2022, **457**, 214389.
3 R. Du, X. Fan, X. Jin, R. Hübner, Y. Hu and A. Eychmüller, *Matter*, 2019, **1**, 39–56.
4 N. Leventis, N. Chandrasekaran, A. G. Sadekar, C. Sotiriou-Leventis and H. Lu, *J. Am. Chem. Soc.*, 2009, **131**, 4576–4577.
5 X. Jiang, R. Du, R. Hübner, Y. Hu and A. Eychmüller, *Matter*, 2021, **4**, 54–94.
6 C. N. Sisk and L. J. Hope-Weeks, *J. Mater. Chem.*, 2008, **18**, 2607–2610.
7 A. E. Gash, J. H. Satcher and R. L. Simpson, *J. Non-Cryst. Solids*, 2004, **350**, 145–151.
8 Y. P. Gao, C. N. Sisk and L. J. Hope-Weeks, *Chem. Mater.*, 2007, **19**, 6007–6011.
9 B. Cai, D. Wen, W. Liu, A. K. Herrmann, A. Benad and A. Eychmüller, *Angew. Chem., Int. Ed.*, 2015, **54**, 13101–13105.
10 R. Poreddy, C. Engelbrekt and A. Riisager, *Catal. Sci. Technol.*, 2015, **5**, 2467–2477.
11 D. Gamarra, A. L. Cámara, M. Monte, S. B. Rasmussen, L. E. Chinchilla, A. B. Hungría, G. Munuera, N. Gyorffy, Z. Schay, V. C. Corberán, J. C. Conesa and A. Martínez-Arias, *Appl. Catal., B*, 2013, **130–131**, 224–238.
12 J. Li, Y. Wu, Y. Qin, M. Liu, G. Chen, L. Hu, W. Gu and C. Zhu, *Chem. Commun.*, 2021, **57**, 13788–13791.
13 R. Baghi, G. R. Peterson and L. J. Hope-Weeks, *J. Mater. Chem. A*, 2013, **1**, 10898–10902.
14 Y. Bi, H. Ren, L. He, Y. Zhang, S. He and L. Zhang, *Mater. Lett.*, 2015, **139**, 205–207.
15 A. Du, B. Zhou, J. Shen, S. Xiao, Z. Zhang, C. Liu and M. Zhang, *J. Non-Cryst. Solids*, 2009, **355**, 175–181.
16 A. Martínez-Lázaro, L. A. Ramírez-Montoya, J. Ledesma-García, M. A. Montes-Morán, M. P. Gurrola, J. A. Menéndez, A. Arenillas and L. G. Arriaga, *Materials*, 2022, **15**, 1422.
17 X'Pert HighScore Plus Software, v3.0e, PANalytical B. V., Amelo, The Netherlands, 2012.
18 H. Ohshima, *Electrical Phenomena at Interfaces and Biointerfaces: Fundamentals and Applications in Nano-, Bio-, and Environmental Sciences*, 2012, vol. 27.
19 R. Du, Y. Hu, R. Hübner, J.-O. Joswig, X. Fan, K. Schneider and A. Eychmüller, *Sci. Adv.*, 2019, **5**, eaaw4590.
20 R. Zhou, Y. Zheng, D. Hulicova-Jurcakova and S. Z. Qiao, *J. Mater. Chem. A*, 2013, **1**, 13179–13185.